miR-135a-3p as a promising biomarker and nucleic acid therapeutic agent for ovarian cancer

Satoshi Fukagawa[a,3*], Kohei Miyata[a,c*], Fusanori Yotsumoto[a], Chihiro Kiyoshima[a,c], Sung Ouk Nam[a], Haruchika Anan[a], Takahiro Katsuda[a], Daisuke Miyahara[a], Masaharu Murata[a], Hiroshi Yagi[d], Kyoko Shirota[a], Shin'ichiro Yasunaga[b,c], Kiyoko Kato[d], and Shingo Miyamoto[a**]

[a] Department of Obstetrics & Gynecology, and [b]Department of Biochemistry, Faculty of Medicine, and [c]Central Research Institute for Advanced Molecular Medicine, Fukuoka University, Japan. [d]Department of Obstetrics and Gynecology, Faculty of Medicine, Kyusyu University, Fukuoka, Japan.

* Both authors contributed equally to this work.

****Correspondence to:** Shingo Miyamoto, Department of Obstetrics & Gynecology, Faculty of Medicine, Fukuoka University, 7-45-1 Nanakuma, Jonan-ku, Fukuoka 814-0180, Japan. Phone: +81-92-801-1011; Fax: +81-92-865-4114; E-mail: smiya@cis.fukuoka-u.ac.jp

The precise word count of the manuscript：4909 words

Number of Tables：2

Number of Supplementary Tables：**3**

Number of Figures：5

Number of Supplementary Figures：**4**

Key words: miR-135a, biomarker, molecular target, nucleic acid therapy, ovarian cancer

Summary

Ovarian cancer is the most lethal gynecologic malignancy. Recently, several molecularly targeted anticancer agents have been developed for ovarian cancer; however, its prognosis has remained extremely poor. The development of molecularly targeted therapy, as well as companion diagnostics, is required to improve outcomes for patients with ovarian cancer. In this study, to identify microRNAs involved in the progression of ovarian cancer we analyzed serum microRNAs in patients with ovarian cancer using microRNA array and qRT-PCR and examined the anticancer properties of microRNA expression in ovarian cancer cells. In patients with ovarian cancer, high expression of miR-135a-3p in serum samples was significantly associated with favorable clinical prognosis. Expression of miR-135a-3p was significantly decreased in patients with ovarian cancer compared with patients with ovarian cysts or normal ovaries. In SKOV-3 and ES-2 human ovarian cancer cells, enhanced expression of miR-135a-3p induced drug sensitivity to cisplatin and paclitaxel and suppressed cell proliferation and xenograft tumor growth. These findings suggest that miR-135a-3p may be considered as a biomarker and a therapeutic agent in ovarian cancer.

(172 words)

1. Introduction

microRNAs (miRNAs) are small non-coding RNAs (18–22 nt) that modulate gene expression. They contribute to many biological processes including cell proliferation, differentiation, and death, and are also involved in pathologies such as cancer, diabetes, cardiovascular, and gynecologic diseases (1-3). miRNAs are present in exosomes in various biofluids such as plasma, serum, urine, semen, menstrual blood, and amniotic fluid, and consequently have been proposed as ideal candidates for disease biomarkers (4). Recently, they have also been proposed as drug targets for many human diseases (5-7).

Ovarian cancer, the most lethal malignancy in gynecologic oncology, is characterized by an extremely poor prognosis from the extensive spread of ovarian cancer cells into the peritoneal cavity (8). Cytoreductive surgery and the introduction of platinum plus taxane-based chemotherapies in the past decade have improved survival in patients with epithelial ovarian cancer (9,10). In the ICON7 trial, standard chemotherapy with bevacizumab did not increase overall survival in patients with newly diagnosed ovarian cancer, although it did improve progression-free survival (PFS) and peritoneal fluid retention (11). In clinical trials, PARP inhibitors did not improve overall survival, whereas PFS was significantly prolonged (12). Accordingly, the development

of molecularly targeted therapeutics and their diagnostic companion tests is required to improve these poor outcomes.

Many reports have investigated alterations in miRNA levels as biomarkers in ovarian cancer (13-16). Currently, inconsistencies in results do not support the use of miRNA as a diagnostic tool in tissue or serum specimens from patients with ovarian cancer. In many studies, miRNA expression in ovarian cancer tissue was compared with that in normal ovarian tissue. However, typically, the ovarian epithelium was not microdissected or scraped, meaning that the difference in miRNA expression between ovarian cancer tissue and ovarian stroma was evaluated, even though ovarian stroma compromises more than 95% of the ovarian tissue in normal specimens (14). Moreover, because of major differences in serum miRNA expression between malignant and benign tumor status, comparisons of normal versus tumor tissue are considered inadequate to identify miRNAs regulating carcinogenesis. To explore key miRNAs as biomarkers for cancer progression, proper selection and high quality tissue or serum specimens are essential.

In this study, to identify candidate miRNAs as biomarkers and for therapeutic intervention in the progression of ovarian cancer, we performed miRNA array analysis of sera between patients with poor and favorable prognosis and evaluated the clinical

significance of these miRNAs and tumor properties after their transfection into ovarian cancer cells. Our data identified miR-135a-3p as a miRNA that regulates tumor potential through modulating drug sensitivity and tumor growth.

2. Material and methods

2.1. Serum, peritoneal fluid, and tissue samples

All clinical samples were obtained from Fukuoka University Hospital (n=88, Fukuoka, Japan) or Kyusyu University Hospital (n=98, Fukuoka, Japan). Serum samples were placed at 4°C no more than 24 h after collection and separated from clots by centrifugation at 3,000 rpm for 20 min at 4°C. Peritoneal fluids and tissue samples were collected at primary surgery and placed on ice immediately. Peritoneal fluids were centrifuged at 3,000 rpm for 20 min at 24°C to separate debris within 1 h of collection. Tissue samples were soaked in RNAlater solution (Life Technologies) and incubated at 4°C overnight (for ≤24 h). All sera, peritoneal fluids, and tissue samples were stored at −80°C for further RNA extraction.

Twelve patients with ovarian cancer (Supplementary Table 1) were enrolled for miRNA array analysis. They were divided into two groups: the poor prognosis group (group A) consisted of six patients who had recurrence of ovarian cancer within 6

months after completion of primary treatment including both platinum and taxane, and the favorable prognosis group (group B) included six patients with ovarian cancer who had no recurrence or recurrence more than 6 months after completion of primary treatment containing both platinum and taxane.

For real-time PCR (qPCR) of the miRNAs, serum obtained from 98 patients (group C) with ovarian cancer (Supplementary Table 2) was analyzed to assess the relationship between miRNA expression and PFS. To assess expression of miR-135a-3p and its target genes, serum and tissue samples were simultaneously examined in 47 patients with ovarian cancer (group D; Supplementary Table 2). For 17/47 patients, miR-135a-3p in peritoneal fluid was also examined using qPCR. Additionally, miR-135a-3p expression was also examined as controls in sera from seven patients with benign gynecologic diseases (mean age ± SD, 65.2 ± 4.8), in sera and peritoneal fluids from 24 patients with benign ovarian cysts (age: 38.0 ± 17.6), in tissues from five patients with endometrial cancer in clinical stage I (group E; Supplementary Table 2), and in five RNA samples of normal ovary tissue obtained from OriGene Technologies (Catalog No: CR561675, CR561070, CR561721, CR560512, CR562355; Kanagawa, Japan) .

The present study was approved by the Ethics Committee of Fukuoka

University Hospital (Fukuoka, Japan) and Kyusyu University Hospital (Fukuoka, Japan). All individuals provided written informed consent. Sera, peritoneal fluid, or tissue samples from ovarian cancer patients were collected from 2009–2015 at Fukuoka University and Kyusyu University. Clinical and pathologic information for ovarian cancer patients was collected from clinical records. Tumors were staged using the International Federation of Gynecology and Obstetrics (FIGO) staging system. All ovarian cancer patients had been diagnosed histopathologically without radiotherapy or chemotherapy prior to study participation. These patients included newly diagnosed cases and those undergoing follow-up.

2.2. Total RNA extraction

Total RNA was isolated from sera and peritoneal fluids using QIAzol reagent (Qiagen, Tokyo, Japan) and the miRNeasy Serum/Plasma Kit (Qiagen). Briefly, 300 µl of serum or peritoneal fluids sample was mixed with 1.5 ml of Qiazol Lysis Reagent and incubated at room temperature for 5 min. As a spike-in control, 3.5 µl of 1.6×10^8 copies/µl miR-39-3p from *Caenorhabditis elegans* (Cel-miR-39-3p) was added. RNA was purified according to the manufacturer's protocol and eluted in 38 µl of RNase-free water. Total RNA was isolated from tissues using TRIzol reagent (Invitrogen) according

to the manufacturer's protocol. RNA concentrations and 260 to 280 nm absorbance ratios were measured using a Nano Drop 1000 spectrophotometer (NanoDrop Technologies, Wilmington, DE).

2.3. Reverse transcription (RT) and qPCR

For cDNA generation for miRNAs, 5 µl of total RNA was used for each RT reaction with specific primers for miR-135a-3p, miR-630, miR-1207, Cel-miR-39-3p, and RNU6B, according to the manufacturer's protocol (Life Technologies). For cDNA generation from mRNA, total RNA from tissues was reverse transcribed using PrimeScript II reverse transcriptase (Takara Bio, Otsu, Shiga, Japan) according to the manufacturer's protocol. The RT product was stored at −80°C.

qPCR was subsequently performed with an ABI Prism 7500 Fast Real-Time PCR system (Applied Biosystems, Foster City, CA) in a 15- or 20-µl reaction with TaqMan Universal Master Mix (Applied Biosystems). Amplification was carried out by denaturation at 95°C for 10 min, followed by 40 cycles of 95°C for 15 s and 60°C for 60 s.

Exponential processes (Ct-values) of miRNAs from serum and peritoneal fluids were converted to linear comparisons relative to the control group and normalized

to the spike-in Cel-miR-39-3p using $2^{-\Delta\Delta Ct}$ methods. Gene expression was analyzed using the difference in cycle threshold ($2^{-\Delta\Delta Ct}$) method. Ct values of tissue miRNA were normalized to RNU6B, and those of mRNA were normalized to GAPDH as internal controls. ΔΔCT values were plotted and statistical analysis was performed using GraphPad Prism (GraphPad Software, CA, USA). The TaqMan primer and probes (Applied Biosystems) used were as follows: miR-135a-3p, 002232; miR-630, 001563; miR-1207, 002826; cel-miR-39; 000200; RNU6B, 001093; BIRC3, Hs00985031_g1; GABRA3, Hs00968132_m1; SPANXB1/2, Hs02387419_gH; TMPRss15, Hs00160491_m1; NCAM2, Hs00189850_m1; SYT4, Hs01086433_m1; C9orf152, Hs00418117_m1; IL1RAP, Hs00895050_m1; RERG, Hs01556349_m1; PAIP1, Hs01925976_s1; PPP2R2B, Hs00270227_m1; and GAPDH, Hs02758991.

2.4. miRNA microarray and expression array analysis

miRNA microarray profiling was carried out using Agilent Human miRNA Microarray (Agilent Technologies, Japan), containing probes for 1,523 human and 364 viral miRNAs from the Sanger database. Total RNA was extracted as above and purified using the SV Total RNA Isolation System (Promega). cRNA was amplified and labelled with Cy3 using a Low input Quick Amp Labeling Kit (Agilent Technologies). cRNA was

hybridized to a 60 K 60-mer oligomicroarray (SurePrint Human miRNA Microarray Release 16.0, 8 × 60 K; Agilent Technologies) according to the manufacturer's instructions. Hybridized microarray slides were scanned using an Agilent scanner. Relative hybridization intensities and background hybridization values were calculated using Feature Extraction Software version 9.5.1.1 (Agilent Technologies). Scanned images were analyzed with Feature Extraction Software 9.5.1.1 (Agilent) using default parameters to obtain background subtracted and spatially detrended Processed Signal intensities. Raw signal intensities and flags for each probe were calculated from hybridization intensities and spot information according to procedures recommended by Agilent Technologies using Flag criteria in GeneSpring Software. The complete data set may be accessed at NCBI-Gene Expression Omnibus (accession GSE79943).

Expression array profiling was carried out using the Affymetrix Human Gene 2.0 ST Array as described in the manufacturer's protocol. The analysis was conducted using SKOV-3 and ES-2 cells with forced expression of miR-135a using an expression vector. Total RNA extraction was performed using the RNeasy Plus Mini Kit (Qiagen) according to the manufacturer's instructions. cDNA synthesis, amplification, and labeling with biotin were performed with the WT PLUS Reagent Kit (Affymetrix). RNA Integrity Number (RIN) values of extracted RNA were determined with an Agilent 2100

Bioanalyzer (Agilent Technologies). To ensure optimal data quality, only samples with RIN ≥9.0 were included in the analysis. Following fragmentation, 4.7 μg of cDNA was hybridized on the GeneChip Human Gene 2.0 ST Array using the GeneChip Hybridization Oven 645. GeneChips were washed and stained in the GeneChip Fluidics Station 450. GeneChips were scanned using the GeneChip Scanner 3000 7G. Data were analyzed with Expression Console v1.4 (Affymetrix) and Transcriptome Analysis Console v3.0 (Affymetrix). Robust multichip average (RMA) was used as a summarization algorithm. Value definition was log2 GC-RMA signal. Microarray data were analyzed using GeneSpring software. The complete data set may be accessed at NCBI-Gene Expression Omnibus (accession GSE 84723).

2.5. Cell culture

Human ovarian cancer cell lines SKOV-3, ES-2, OVCAR-3, and RMG-1 were obtained from the American Type Culture Collection (ATCC, Manassas, VA). Cells were cultured in RPMI-1640 medium supplemented with 10% fetal bovine serum (FBS; ICN Biochemicals, Irvine, CA), 100 U/ml penicillin G, and 100 μg/ml streptomycin (Invitrogen, Carlsbad, CA) in a humidified atmosphere of 5% CO_2 at 37°C.

2.6. Generation of stably transfected cell lines

The Hsa-miR-135a coding region was PCR-amplified from 293T genomic DNA using the following primers: miR-135a_Fw_735, 5′-gcgaagcttAGGCCTCGCTGT TCTCTATGG-3′; miR-135a_Rv, 5′-catggatccTGTCCCCGCCGTGCGCCACGG-3′. The fragment was inserted into *Hind*III/*Bam*HI sites of the pmR-ZsGreen-1 (Takara, Clontech) vector. Expression vectors for pmR-ZsGreen1/miR-135a or pmR-ZsGreen1 (as control) were transfected into SKOV-3, ES-2, OVCAR-3, and RMG-1 cells using Lipofectamine 2000 (Invitrogen). At 48–72 h post-transfection, the culture medium was changed to RPMI-1640 supplemented with 10% FBS and puromycin to select transfected cells.

2.7. WST-8 assay

The effect of miR-135a-3p on SKOV-3, ES-2, OVCAR-3, or RMG-1 cell viability was determined using the WST-8 assay kit (Cell Counting Kit-8, Dojindo, Kumamoto, Japan). Stable transfected SKOV-3 and ES-2 cell lines were seeded in 96-well plates and allowed to grow for 48 h. Freshly prepared anticancer drugs paclitaxel (PTX; 10 nM, 100 nM, or 1000 nM) and cisplatin (CDDP; 10 μM, 20 μM, 30

μM, or 100 μM) were added to each well. After 48 h, WST-8 was added to each well for 1 h before the first measurement. Absorbance at 450 nm was measured using a microplate reader according to the manufacturer's instructions.

2.8. Antitumor effects of miR-135a-3p in a mouse xenograft model

Subconfluent cell cultures were detached from plates with trypsin-EDTA. A total volume of 250 μl containing 1×10^6 cells suspended in serum-free RPMI-1640 was injected subcutaneously into 4-week-old nude mice (Charles River Laboratories Japan Inc., Yokohama, Japan). To assess the inhibitory effects of miR-135a-3p on tumor growth, cells transfected with miR-blank or miR-135a-3p were injected subcutaneously and the tumor volume was estimated from two-dimensional tumor measurements as follows: tumor volume (mm^3) = (length×$width^2$)/2. The animal protocol was approved according to the guidelines of the Animal Care of Fukuoka University (Approval No. 1306662) and the Ethics committee. Animals were observed daily. Humane endpoints were defined as loss of more than 10% of body mass, tumor diameter greater than 20 mm, or inability to ambulate or rise for food and water. If animals reached these endpoints they were euthanized by exsanguination. Animal surgery and euthanasia

using decapitation were performed under inhalation (isoflurane) anesthesia, and all efforts were made to minimize suffering.

2.9. Target gene profiling

Microarray data were analyzed using GeneSpring software. A fold change <–3.0 or >3.0 was considered statistically significant. Hierarchical clustering analysis was used to organize the genes based on similarities in expression profiles.

Target prediction for miR-135a-3p was also performed using the algorithms Targetscan (http://www.targetscan.org/vert_71/), miRDB (http://mirdb.org/miRDB/), and miRanda (http://www.microrna.org/microrna/home.do) in terms of base sequence. All prediction processes were conducted using custom-written executable files that computed the parameters between miRNAs and mRNAs based on inherent algorithms and set thresholds. The thresholds for the algorithms were context score ≤–0.4 for Targetscan; Target score ≥60 for miRDB; and seed misSVR score >–1.25 for miRanda.

2.10. Statistical analysis

All experiments were carried out in triplicate and quantitative values were expressed as means ± SEM. Cutoff values of miR-135a-3p, miR-630, and miR-1207

expression were taken as the medians of expression levels in serum from 98 patients with ovarian cancer. The statistical significance of differences among the groups was assessed using the Mann–Whitney U test. Correlation was tested and presented as Pearson's correlation coefficient (r). The survival fraction was calculated by the Kaplan–Meier test with 95% confidence intervals computed by the asymmetrical method using the log-rank test. A value of $P<0.05$ was considered statistically significant. Analysis was performed using GraphPad Prism (GraphPad Software, La Jolla, CA).

3. Results

3.1. Serum miRNA expression profiles associated with prognosis in ovarian cancer patients

To identify serum biomarkers associated with clinical prognosis of ovarian cancer, we compared serum miRNA expression changes between group A (poor prognosis) and group B (favorable prognosis). Three miRNAs, miR-135a-3p, miR-630, and miR-1207, that showed significant differences in the miRNA expression index in serum samples between Group A and B were identified using miRNA array analysis (Table 1). To assess their clinical significance, we calculated the median value for each

in 98 ovarian cancer patients and examined PFS in patients with low or high expression of miRNA based on each median value. The median expression index of miR-135a-3p, miR-630, and miR-1207 was 0.406, 0.000403, and 0.211, respectively, with the former markedly enhanced compared with the other two (Supplementary Figure 1). Patients harboring high miR-135a-3p expression showed a significantly favorable prognosis compared with those harboring low expression; in contrast, expression of miR-630 or miR-1207 was not associated with clinical prognosis (Figure 1). These results suggest that miR-135a-3p might be considered a biomarker in ovarian cancer.

3.2 Clinical significance of miR-135-3p in ovarian cancer patients

To provide clinical insights into miR-135a-3p expression in ovarian cancer, we examined the miR-135a-3p expression index in serum, peritoneal fluid, or tissue samples of patients with ovarian cancer, ovarian cysts, normal ovaries, or endometrial cancer. This serum index was significantly decreased in ovarian cancer patients compared with those with ovarian cysts or normal ovaries (Figure 2A), while the tissue sample index was significantly reduced in ovarian cancer patients compared with those with normal ovaries (Figure 2B), and the peritoneal fluid sample expression index was significantly suppressed in ovarian cancer patients compared with those with ovarian cysts or early endometrial cancer (Figure 2C). In any patient, the miR-135a-p

expression level in peritoneal fluid samples was approximately 10 times higher than in serum samples, and 100 times higher than in tissue samples. In 47 ovarian cancer patients, the serum miR-135a-3p expression index was significantly correlated with that in tissue samples ($P<0.05$, $r=0.3671$) (Figure 2D). In 17/47 ovarian cancer patients, the serum miR-135a-3p expression index was also significantly associated with that in peritoneal samples ($P<0.05$, $r=0.5703$) (Figure 2E). However, in all 47 ovarian cancer patients, the serum miR-135a-3p expression index was not correlated with the value of CA125 in serum samples (Supplementary Figure 2). These findings suggest that miR-135a-p is produced in the cells and excreted into the peritoneal fluid, and may contribute to cancer progression.

3.3. Contribution of miR-135a-p to cancer progression

To gain insights into miR-135a-p as a therapeutic target for ovarian cancer, we examined tumor activity including cell proliferation, chemosensitivity, and tumor formation after transfection of miR-135a-3p or miR-blank into ovarian cancer cells. Cells transfected with miR-135a-3p had marked expression of mR-135a-3p, compared with cells transfected with miR-blank (all $P<0.05$) (Figure 3A). Transfection of miR-135a-3p into SKOV-3, ES-2, OVCAR-3, or RMG-1 cells significantly suppressed cell viability compared with miR-blank transfection (all $P<0.05$) (Figure 3A).

Transfection of miR-135a-3p into SKOV-3 or ES-2 cells significantly reduced cell viability for each concentration of CDDP or paclitaxel compared with transfection of miR-blank (all $P<0.05$) (Figure 3B). In SKOV-3 cells, miR-135a-3p transfection completely blocked tumor formation compared with miR-blank (Figure 3C). In ES-2 cells, transfection of miR-135a-3p markedly suppressed tumor growth compared with miR-blank (Figure 3C). These findings indicate that miR-135a-3p attenuates malignant properties of ovarian cancer cells, including cell proliferation, drug sensitivity, and tumor formation, suggesting that miR-135a-3p itself may be considered a therapeutic agent in nucleic acid medicine for ovarian cancer.

3.4. Identification of genes regulated by miR-135a-3p expression in ovarian cancer

To identify the genes and specific pathways altered by miR-135a-3p expression, we examined gene expression changes between cells transfected with miR-135a-3p and miR-blank and then analyzed the specific pathways affected. Comparison of common gene expression changes in SKOV-3 and ES-2 cells after transfection with miR-135a-3p or miR-blank identified six genes that showed >3-fold expression changes in cells transfected with miR-135a-3p compared with miR-blank as candidate targeted genes (Group 1) (Figure 4A and Table 2). Additionally, genes showing >2-fold change between cells transfected with miR-135a-3p and miR-blank were also analyzed

according to specific pathways. A total of 20 genes showed >2-fold upregulation and 58 genes showed >2-fold downregulation in cells transfected with miR-135a-3p compared with miR-blank. However, analysis of specific pathways revealed that no more than three genes were involved in the same pathway.

To confirm the expression of the six genes showing >3-fold change in expression in miR-135a-3p-transfected cells, we examined the expression index of each gene in SKOV-3 or ES-2 cells transfected with miR-135a-3p or miR-blank using RT-PCT. Expression of all six genes was reduced by the introduction of miR-135a-3p compared with miR-blank in both ovarian cancer cell lines (all $P<0.05$) (Figure 4B). To verify the clinical importance of these genes in ovarian cancer, we examined their expression in tissue samples of 20/47 patients with ovarian cancer and five patients with normal ovaries using RT-PCR. For five genes in Group 1, the expression index of *BIRC3*, *GAGRA3*, and *SPANXB1/SPANXB2* was significantly increased in ovarian cancer patients compared with patients with normal ovaries (all $P< 0.05$), whereas no expression of *NCAM2* or *TMPRSS15* was found in ovarian cancer patients or those with normal ovaries (Figure 5A).

Through combination analysis of Targetscan, miRDB, and miRanda for the sequence of miR-135a-3p, six genes were identified as theoretical targets for

miR-135a-3p (Group 2) (Supplementary Figure 3 and Supplementary Table 3). To assess the clinical importance of these genes in ovarian cancer we examined their expression as described above for the six genes. *PPP2R2B* expression was significantly increased in ovarian cancer patients compared with patients with normal ovaries ($P<0.05$) (Figure 5B). No significant difference was observed in the expression of *SYT4*, *IL1RAP*, *RERG*, *C9orf152*, or *PAIP1* between ovarian cancer patients and those with normal ovaries (Figure 5B). According to these findings, miR-135a-3p appears to directly regulate *PPP2R2B* expression and indirectly regulate that of *BIRC3*, *GAGRA3*, or *SPNAXB1/SPANXB2*, resulting in the progression of ovarian cancer.

4. Discussion

In this study, we demonstrated that miR-135a-3p is abundantly present in cells and biofluids, including serum and peritoneal fluid, and that miR-135a-3p suppresses malignant properties in ovarian cancer. It is therefore plausible that miR-135a-3p, which is already recognized as a serum biomarker and a nucleic acid agent for cancer therapy, is a promising miRNA for the treatment of ovarian cancer.

miR-135a-3p expression in peritoneal fluid was enriched up to 100-fold compared with that in cells or sera of any patient. Additionally, its expression was

attenuated with the increase in peritoneal fluid during ovarian cancer progression. Accordingly, it is possible that miR-135a-3p affects the circulation of peritoneal fluid. Many studies have investigated the relationship between miR-135a-5p and cancer (17-23), but few concern miR-135a-3p (24,25). miR-135a-5p has often been reported to function as a potential tumor suppressor (17-23). In prostate cancer cells, miR-135a-3p was shown to mimic the enhanced apoptosis induced by death receptor 5 with respect to increased PARP cleavage, Bax expression, and the number of TUNEL-positive cells following co-treatment with Tanshinone I and TRAIL (25). Our present study indicates that miR-135a-3p may also have antitumor activities in ovarian cancer. Human miR-135a is encoded by two genes located on different chromosomes that produce identical active sequences (chromosomes 3 and 12 for miR-135a1 and miR-135a2, respectively). Additionally, miR-135a-3p and miR-135a-5p are produced from the same transcript. Although contradictory results have been reported concerning the effects of miR-135a-3p and miR-135a-5p on cancer progression, the genes targeted by miR-135a may themselves be involved in cell growth.

Combination analysis of the miR-135a-3p sequence by Targetscan, miRDB, and miRanda predicted that miR135a-3p might directly regulate the expression of six genes (Supplementary Figure 4). We showed that *PPP2R2B* expression was

significantly increased in ovarian cancer compared with normal ovaries. *PPP2R2B* encodes a regulatory subunit of protein phosphatase 2A, which has been implicated in breast tumorigenesis and progression (26-28). PPP2R2B was reported to contribute to HER-2 signaling and enhanced expression of estrogen receptor in breast cancer (26, 27). Our screen of transfected ovarian cancer cells identified five genes as putative targets for miR-135a-3p. We further showed that the expression of *BIRC3*, *GABRA3*, and *SPANXB1/SPANXB2* was significantly upregulated in ovarian cancer compared with normal ovaries. BIRC3 belongs to the inhibitor of apoptosis family of proteins and plays pivotal roles in the regulation of nuclear factor-kB signaling and apoptosis (29). Various somatic alterations of *BIRC3* have been identified in lymphoid malignancies and many epithelial tumors, including ovarian cancer (30, 31). GABA is an inhibitory neurotransmitter that functions through two types of GABA receptors: ionotropic receptors including GABAA and GABAC receptors, and the metabotropic GABAB receptor (32, 33). GABRA3, of the GABAA group of receptors, is normally expressed in adult brain, and is inversely correlated with breast cancer survival; it activates the AKT pathway to promote breast cancer cell migration, invasion, and metastasis (34). GABRA3 enhances lymphatic metastasis in lung adenocarcinoma through activating the JNK/AP-1 signaling pathway (35). The testis-specific gene *SPANXB* is normally

expressed only in spermatozoa. Although sporadic SPANXB expression has previously been demonstrated in cancer cell lines and hematologic malignancies, the function of *SPANXB* or related genes is poorly understood (36, 37). We also showed that 58 genes were suppressed and 30 upregulated in our gene profiling, suggesting that miR-135a-3p can directly or indirectly regulate the expression of many oncogenic or suppressive genes in ovarian cancer progression.

DNA and RNA are simple linear polymers that have moved into the realm of stand-alone therapeutic agents for a variety of human diseases (38). Several types of RNA molecules with complex biological functions, including mRNA, transfer RNA, miRNA, and short interfering (si)RNA, have been discovered (38), while major chemical modifications in siRNA and miRNA have been identified, including the ribose 2′-OH group modification, locked and unlocked nucleic acids, and phosphorothioate modification, leading to a diverse range of therapeutic applications for human diseases (39). On the basis of this, clinical trials of siRNA- and miRNA-based drugs have already been initiated (39, 40). In this study, miR-135a-3p can be regarded as an integrated therapeutic agent with multiple targets for ovarian cancer therapy, and is probably associated with the retention of peritoneal fluid, chemoresistance, and tumorigenesis in ovarian cancer. In ovarian cancer patients, the presence of ascites is

essentially treated through management of underlying disease. Once chemoresistance has developed, however, intractable ascites can be a major problem involving several molecules (41). Accordingly, intravenous or subcutaneous administration of miR-135a-3p mimics may improve the clinical prognosis in peritonitis carcinomatosa induced by ovarian cancer through the enhancement of chemosensitivity or the reduction of ascites.

In conclusion, the iR-135a-3p expression index is suitable for application as a biomarker in treatment of ovarian cancer, and miR-135a-3p mimics are promising agents for ovarian cancer therapy.

(4044 words)

Acknowledgements

This work was supported in part by a Grant-in-Aid for Young Scientists (B) (no. 227790536) Challenging Exploratory Research (no. 26670731), Scientific Research (B) (no. 26293362), Scientific Research (C) (no. 23592470), and funds from the Central Research Institute of Fukuoka University (141011); The Center for Advanced Molecular Medicine, Fukuoka University from the Ministry of Education, Culture, Sports, Science and Technology (Tokyo, Japan), a Grant-in-Aid from the Kakihara Science and

Technology Foundation (Fukuoka, Japan); and Princess Takamatsu Cancer Research Fund to S. Miyamoto.

Disclosure Statement

The authors have no conflict of interest.

References

1. Bartel DP. MicroRNAs: genomics, biogenesis, mechanism, and function. Cell. 2004;116(2):281-97.
2. Lewis BP, Burge CB, Bartel DP. Conserved seed pairing, often flanked by adenosines, indicates that thousands of human genes are microRNA targets. Cell. 2005;120(1):15-20.
3. Mendell JT, Olson EN. MicroRNAs in stress signaling and human disease. Cell. 2012;148(6):1172-87.
4. Ha M, Kim VN. Regulation of microRNA biogenesis. Nature reviews Molecular cell biology. 2014;15(8):509-24.
5. Lindow M, Kauppinen S. Discovering the first microRNA-targeted drug. The Journal of cell biology. 2012;199(3):407-12.
6. Hayes J, Peruzzi PP, Lawler S. MicroRNAs in cancer: biomarkers, functions and therapy. Trends in molecular medicine. 2014;20(8):460-9.
7. Pichler M, Calin GA. MicroRNAs in cancer: from developmental genes in worms to their clinical application in patients. British journal of cancer. 2015;113(4):569-73.
8. Tan DS, Agarwal R, Kaye SB. Mechanisms of transcoelomic metastasis in ovarian cancer. The Lancet Oncology. 2006;7(11):925-34.
9. Crawford SC, Vasey PA, Paul J, Hay A, Davis JA, Kaye SB. Does aggressive surgery only benefit patients with less advanced ovarian cancer? Results from an

international comparison within the SCOTROC-1 Trial. Journal of clinical oncology : official journal of the American Society of Clinical Oncology. 2005;23(34):8802-11.
10. Trimble EL, Wright J, Christian MC. Treatment of platinum-resistant ovarian cancer. Expert opinion on pharmacotherapy. 2001;2(8):1299-306.
11. Oza AM, Cook AD, Pfisterer J, Embleton A, Ledermann JA, Pujade-Lauraine E, et al. Standard chemotherapy with or without bevacizumab for women with newly diagnosed ovarian cancer (ICON7): overall survival results of a phase 3 randomised trial. The Lancet Oncology. 2015;16(8):928-36.
12. Wiggans AJ, Cass GK, Bryant A, Lawrie TA, Morrison J. Poly(ADP-ribose) polymerase (PARP) inhibitors for the treatment of ovarian cancer. The Cochrane database of systematic reviews. 2015(5):Cd007929.
13. Katz B, Trope CG, Reich R, Davidson B. MicroRNAs in Ovarian Cancer. Human pathology. 2015;46(9):1245-56.
14. Pal MK, Jaiswar SP, Dwivedi VN, Tripathi AK, Dwivedi A, Sankhwar P. MicroRNA: a new and promising potential biomarker for diagnosis and prognosis of ovarian cancer. Cancer biology & medicine. 2015;12(4):328-41.
15. Li Y, Fang Y, Liu Y, Yang X. MicroRNAs in ovarian function and disorders. Journal of ovarian research. 2015;8:51.
16. Nakamura K, Sawada K, Yoshimura A, Kinose Y, Nakatsuka E, Kimura T. Clinical relevance of circulating cell-free microRNAs in ovarian cancer. Molecular cancer. 2016;15(1):48.
17. Yamada Y, Hidaka H, Seki N, Yoshino H, Yamasaki T, Itesako T, et al. Tumor-suppressive microRNA-135a inhibits cancer cell proliferation by targeting the c-MYC oncogene in renal cell carcinoma. Cancer science. 2013;104(3):304-12.
18. Shi H, Ji Y, Zhang D, Liu Y, Fang P. MiR-135a inhibits migration and invasion and regulates EMT-related marker genes by targeting KLF8 in lung cancer cells. Biochemical and biophysical research communications. 2015;465(1):125-30.
19. Kroiss A, Vincent S, Decaussin-Petrucci M, Meugnier E, Viallet J, Ruffion A, et al. Androgen-regulated microRNA-135a decreases prostate cancer cell migration and invasion through downregulating ROCK1 and ROCK2. Oncogene. 2015;34(22):2846-55.
20. Deng YQ, Yang YQ, Wang SB, Li F, Liu MZ, Hua QQ, et al. Intranasal Administration of Lentiviral miR-135a Regulates Mast Cell and Allergen-Induced Inflammation by Targeting GATA-3. PloS one. 2015;10(9):e0139322.
21. Tribollet V, Barenton B, Kroiss A, Vincent S, Zhang L, Forcet C, et al. miR-135a

Inhibits the Invasion of Cancer Cells via Suppression of ERRalpha. PloS one. 2016;11(5):e0156445.
22. Yao S, Tian C, Ding Y, Ye Q, Gao Y, Yang N, et al. Down-reguation of Kruppel-like factor-4 by microRNA-135a-5p promotes proliferation and metastasis in hepatocellular carcinoma by transforming growth factor-beta1. Oncotarget. 2016.
23. Coarfa C, Fiskus W, Eedunuri VK, Rajapakshe K, Foley C, Chew SA, et al. Comprehensive proteomic profiling identifies the androgen receptor axis and other signaling pathways as targets of microRNAs suppressed in metastatic prostate cancer. Oncogene. 2016;35(18):2345-56.
24. Yang B, Jing C, Wang J, Guo X, Chen Y, Xu R, et al. Identification of microRNAs associated with lymphangiogenesis in human gastric cancer. Clinical & translational oncology : official publication of the Federation of Spanish Oncology Societies and of the National Cancer Institute of Mexico. 2014;16(4):374-9.
25. Shin EA, Sohn EJ, Won G, Choi JU, Jeong M, Kim B, et al. Upregulation of microRNA135a-3p and death receptor 5 plays a critical role in Tanshinone I sensitized prostate cancer cells to TRAIL induced apoptosis. Oncotarget. 2014;5(14):5624-36.
26. Mumby M. PP2A: unveiling a reluctant tumor suppressor. Cell. 2007;130(1):21-4.
27. Wong LL, Chang CF, Koay ES, Zhang D. Tyrosine phosphorylation of PP2A is regulated by HER-2 signalling and correlates with breast cancer progression. International journal of oncology. 2009;34(5):1291-301.
28. Keen JC, Zhou Q, Park BH, Pettit C, Mack KM, Blair B, et al. Protein phosphatase 2A regulates estrogen receptor alpha (ER) expression through modulation of ER mRNA stability. The Journal of biological chemistry. 2005;280(33):29519-24.
29. Gyrd-Hansen M, Meier P. IAPs: from caspase inhibitors to modulators of NF-kappaB, inflammation and cancer. Nature reviews Cancer. 2010;10(8):561-74.
30. Yamato A, Soda M, Ueno T, Kojima S, Sonehara K, Kawazu M, et al. Oncogenic activity of BIRC2 and BIRC3 mutants independent of nuclear factor-kappaB-activating potential. Cancer science. 2015;106(9):1137-42.
31. Jonsson JM, Bartuma K, Dominguez-Valentin M, Harbst K, Ketabi Z, Malander S, et al. Distinct gene expression profiles in ovarian cancer linked to Lynch syndrome. Familial cancer. 2014;13(4):537-45.
32. Watanabe M, Maemura K, Oki K, Shiraishi N, Shibayama Y, Katsu K. Gamma-aminobutyric acid (GABA) and cell proliferation: focus on cancer cells. Histology and histopathology. 2006;21(10):1135-41.

33. Vithlani M, Terunuma M, Moss SJ. The dynamic modulation of GABA(A) receptor trafficking and its role in regulating the plasticity of inhibitory synapses. Physiological reviews. 2011;91(3):1009-22.
34. Gumireddy K, Li A, Kossenkov AV, Sakurai M, Yan J, Li Y, et al. The mRNA-edited form of GABRA3 suppresses GABRA3-mediated Akt activation and breast cancer metastasis. Nature communications. 2016;7:10715.
35. Liu L, Yang C, Shen J, Huang L, Lin W, Tang H, et al. GABRA3 promotes lymphatic metastasis in lung adenocarcinoma by mediating upregulation of matrix metalloproteinases. Oncotarget. 2016.
36. Wang Z, Zhang J, Zhang Y, Lim SH. SPAN-Xb expression in myeloma cells is dependent on promoter hypomethylation and can be upregulated pharmacologically. International journal of cancer. 2006;118(6):1436-44.
37. Wang Z, Zhang Y, Liu H, Salati E, Chiriva-Internati M, Lim SH. Gene expression and immunologic consequence of SPAN-Xb in myeloma and other hematologic malignancies. Blood. 2003;101(3):955-60.
38. Breaker RR, Joyce GF. The expanding view of RNA and DNA function. Chemistry & biology. 2014;21(9):1059-65.
39. Lam JK, Chow MY, Zhang Y, Leung SW. siRNA Versus miRNA as Therapeutics for Gene Silencing. Molecular therapy Nucleic acids. 2015;4:e252.
40. Sridharan K, Gogtay NJ. Therapeutic nucleic acids: current clinical status. British journal of clinical pharmacology. 2016;82(3):659-72.
41. Kipps E, Tan DS, Kaye SB. Meeting the challenge of ascites in ovarian cancer: new avenues for therapy and research. Nature reviews Cancer. 2013;13(4):273-82.

Figure Legends

Figure 1. Progression-free survival in ovarian cancer patients with high or low expression index of miR-135a-3p (A), miR-630 (B), or miR-1207 (C). * $P<0.05$

Figure 2. Clinical significance of miR-135a-3p in patients with ovarian cancer, other

gynecologic diseases, and normal ovary. Expression index of miR-135a-3p in serum samples among patients with ovarian cancer, ovarian cyst, and normal ovary (A). Expression index of miR-135a-3p in tissue samples between patients with ovarian cancer and normal ovary (B). Expression index of miR-135a-3p in peritoneal fluid samples among patients with ovarian cancer, ovarian cyst, and endometrial cancer (C). Expression index of miR-135a-3p between serum and tissue samples in 47 patients with ovarian cancer (D), and between serum and peritoneal fluid samples in 17 patients with ovarian cancer (E). R indicates the correlation index. Data are mean ± SEM, * $P<0.05$

Figure 3. Assessment of antitumor properties of miR-135a-3p in ovarian cancer. Alterations in cell viability and the expression index of miR-135a-3p induced by transfection of miR-135a-3p or miR-blank into SKOV-3, ES-2, OVCAR-3, or RMG-1 cells (A). Alteration in cell viability of SKOV-3 or ES-2 cells transfected with miR-135a-3p or miR-blank in the presence of different concentrations of CDDP or paclitaxel (B). Tumor formation on NOD/SCID mice by SKOV-3 or ES-2 cells transfected with miR-135a-3p or miR-blank (C). Data are mean ± SEM, * $P<0.05$.

Figure 4. Expression changes in genes targeted by miR-135a-3p in ovarian cancer. Gene profiling between SKOV-3 and ES-2 cells transfected with miR-135a-3p or miR-blank (A). Alterations in the expression of each targeted gene in SKOV-3 or ES-2

cells transfected by miR-135a-3p or miR-blank (B). Data are mean ± SEM, * P<0.05.

Figure 5. Alterations in the expression of each targeted gene in patients with ovarian cancer or normal ovary (A). Alterations in the expression of each targeted gene predicted by Targetscan, miRDB, and miRanda in patients with ovarian cancer or normal ovary (B). Data are mean ± SEM, * P<0.05.

Supplementary Figure 1. Alterations in the expression index of miR-135a-3p (A), miR-630 (B), or miR-1207 (C) in 98 patients with ovarian cancer.

Supplementary Figure 2. Relationship between the expression index of miR-135a-3p and serum CA125 in 47 patients with ovarian cancer. R indicates the correlation index. * P<0.05.

Supplementary Figure 3. Alterations in body weight of NOD/SCID mice with xenograft tumors of SKOV-3 or ES-2 cells transfected with miR-135a-3p or miR-blank. * P<0.05.

Supplementary Figure 4. Profiling of genes targeted by miR-135a-3p through prediction using Targetscan, miRDB, and miRanda.

Supplementary Table 1. Clinical characteristics of patients with primary OVCA for microarray analysis.

Supplementary Table 2. Clinical characteristic of the OVCA patients for RT-PCR analysis.

Supplementary Table 3. The target prediction by Tagetscan, miRDB and miRanda (Group 2)

(449 words)

Table 1

miRNAs as a candidate of biomarker in primary OVCA.

Symbol	*P-value*	Fold change
hsa-miR-135a-3p	*0.0104*	0.673
hsa-miR-630	*0.0097*	0.405
hsa-miR-1207	*0.0236*	1.266

Table 2

The target candidate by microarray analysis (Group1)

Gene symbol	Gene name	Fold change
BIRC3	Baculoviral IAP repeat containing 3	-3.3256896
GABRA3	Gamma-aminobutyric acid type A receptor alpha 3	-3.3673131
SPANXB1/2	SPANX family member B1/2	-5.5325503
TMPRSS15	Transmembrane protease, serine 15	-10.862935
NCAM2	Neural cell adhension molecule 2	-11.769233

Strongest positive and negative correlation between the most expressed messenger RNA (top upregulated and downregulated genes). In sequence : Gene symbol, gene name, average fold change expression in cells with miR-135a-3p overexpression compared to miR-blank control.

Figure 1

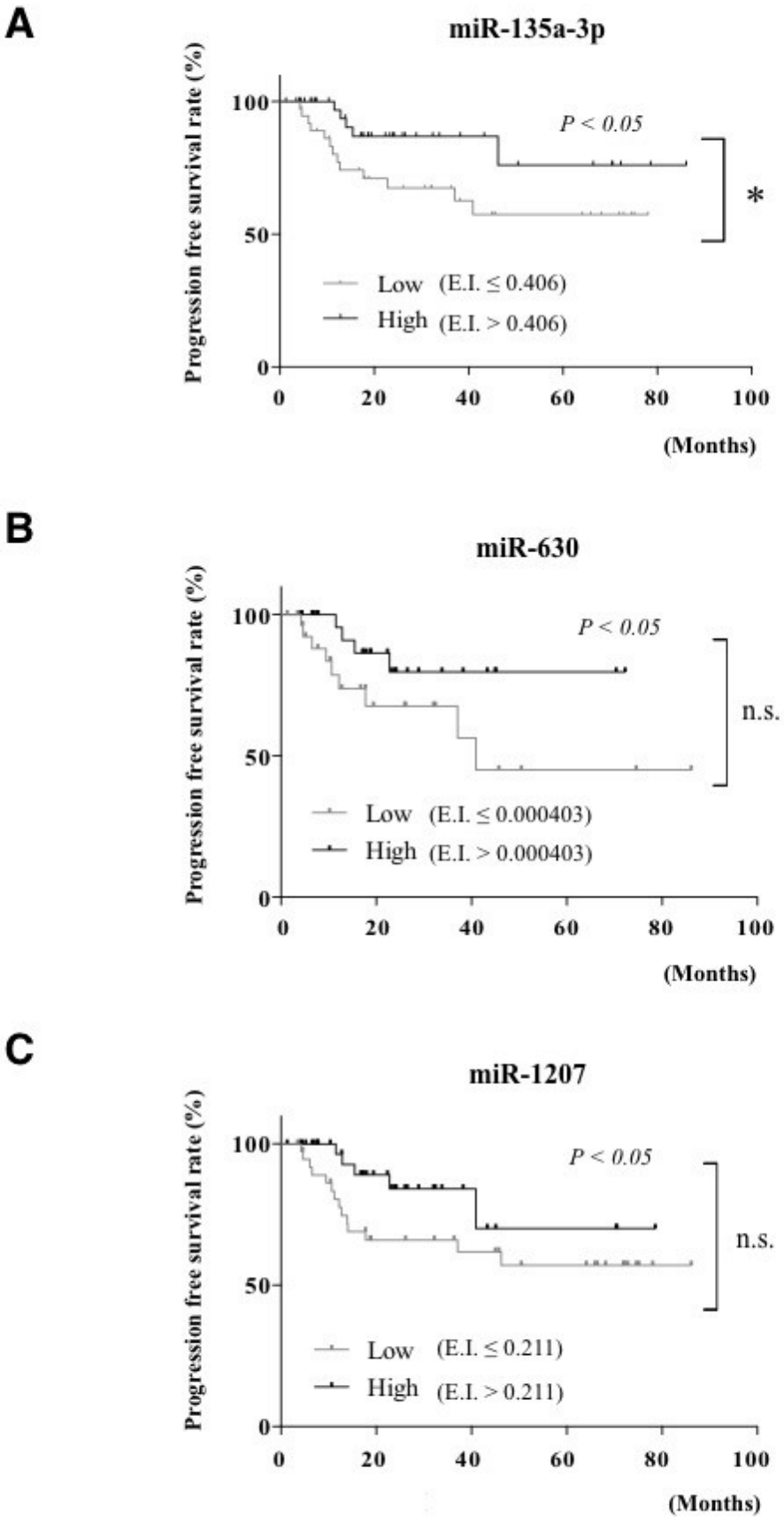
A
miR-135a-3p
Progression free survival rate (%)
100
50
0
P < 0.05
*
Low (E.I. ≤ 0.406)
High (E.I. > 0.406)
0
20
40
60
80
100
(Months)
B
miR-630
Progression free survival rate (%)
100
50
0
P < 0.05
n.s.
Low (E.I. ≤ 0.000403)
High (E.I. > 0.000403)
0
20
40
60
80
100
(Months)
C
miR-1207
Progression free survival rate (%)
100
50
0
P < 0.05
n.s.
Low (E.I. ≤ 0.211)
High (E.I. > 0.211)
0
20
40
60
80
100
(Months)

Figure 2

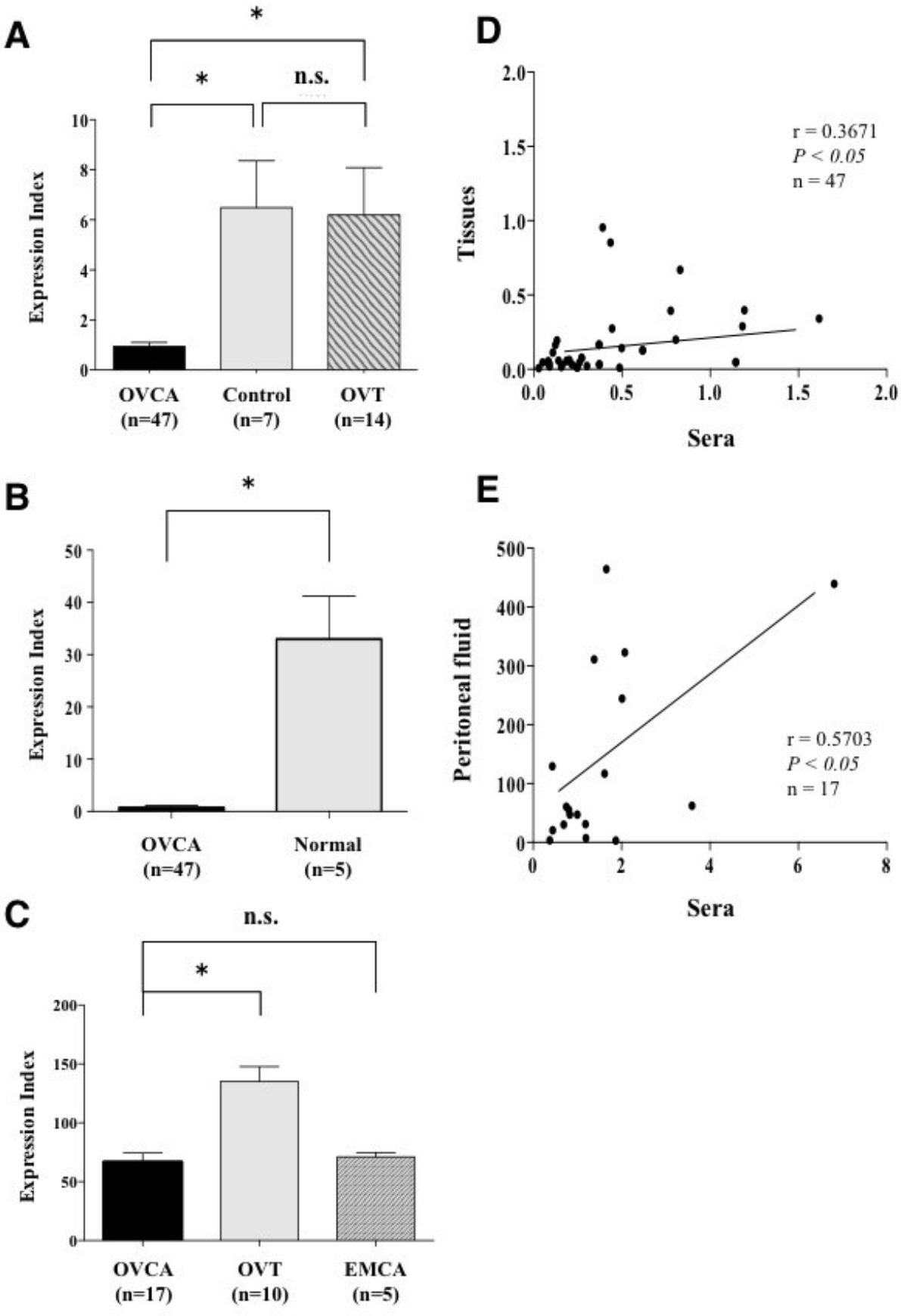
A
*
*
n.s.
Expression Index
10
8
6
4
2
0
OVCA (n=47)
Control (n=7)
OVT (n=14)
B
*
Expression Index
50
40
30
20
10
0
OVCA (n=47)
Normal (n=5)
C
n.s.
*
Expression Index
200
150
100
50
0
OVCA (n=17)
OVT (n=10)
EMCA (n=5)
D
Tissues
2.0
1.5
1.0
0.5
0.0
0.0
0.5
1.0
1.5
2.0
Sera
r = 0.3671
P < 0.05
n = 47
E
Peritoneal fluid
500
400
300
200
100
0
0
2
4
6
8
Sera
r = 0.5703
P < 0.05
n = 17

Figure 3

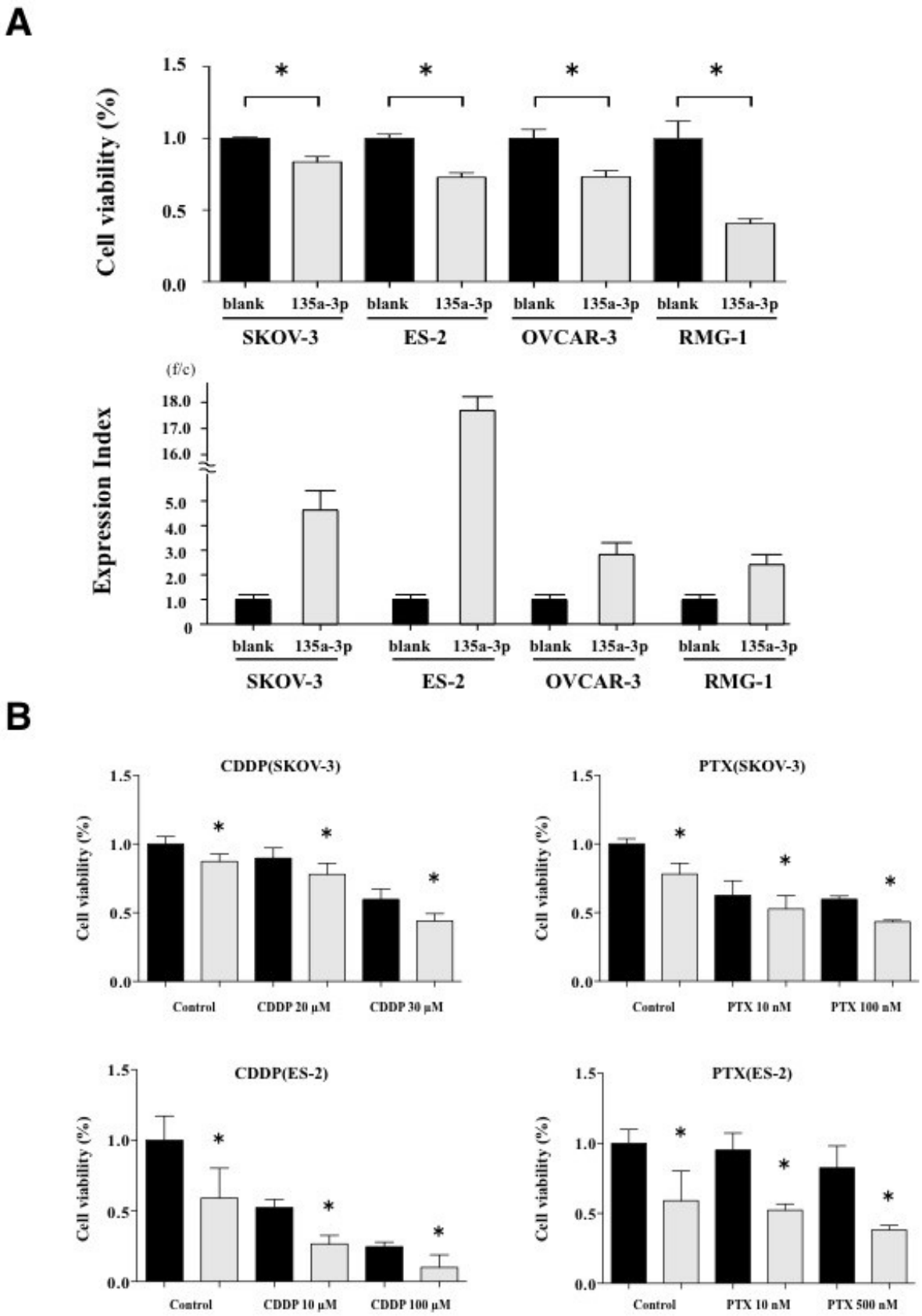
A
Cell viability (%)
1.5
1.0
0.5
0.0
blank
135a-3p
SKOV-3
ES-2
OVCAR-3
RMG-1
Expression Index
(f/c)
18.0
17.0
16.0
5.0
4.0
3.0
2.0
1.0
0
B
CDDP(SKOV-3)
PTX(SKOV-3)
CDDP(ES-2)
PTX(ES-2)
Control
CDDP 20 μM
CDDP 30 μM
PTX 10 nM
PTX 100 nM
CDDP 10 μM
CDDP 100 μM
PTX 500 nM

Figure 3

C

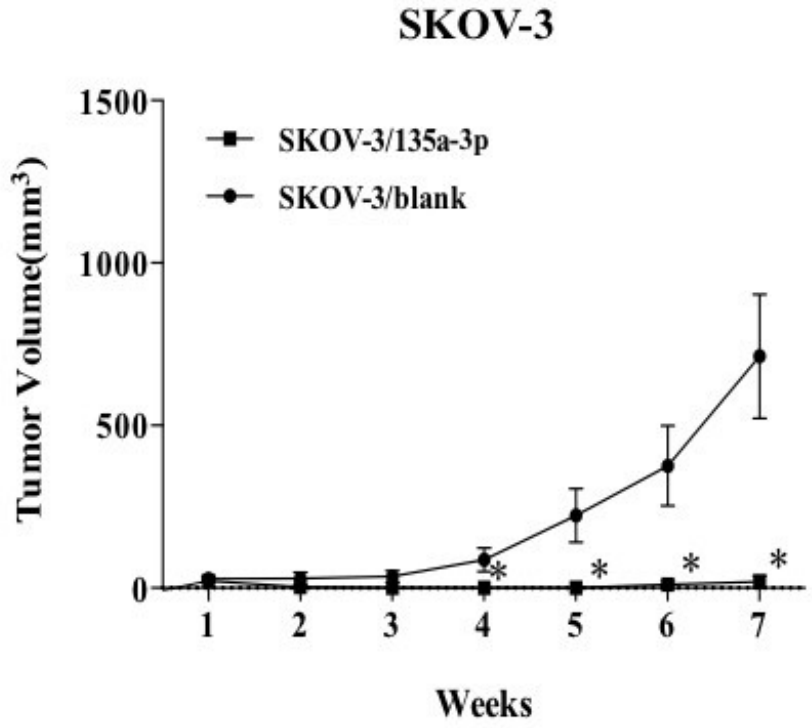
SKOV-3
1500
1000
500
0
Tumor Volume(mm3)
SKOV-3/135a-3p
SKOV-3/blank
*
*
*
*
1
2
3
4
5
6
7
Weeks

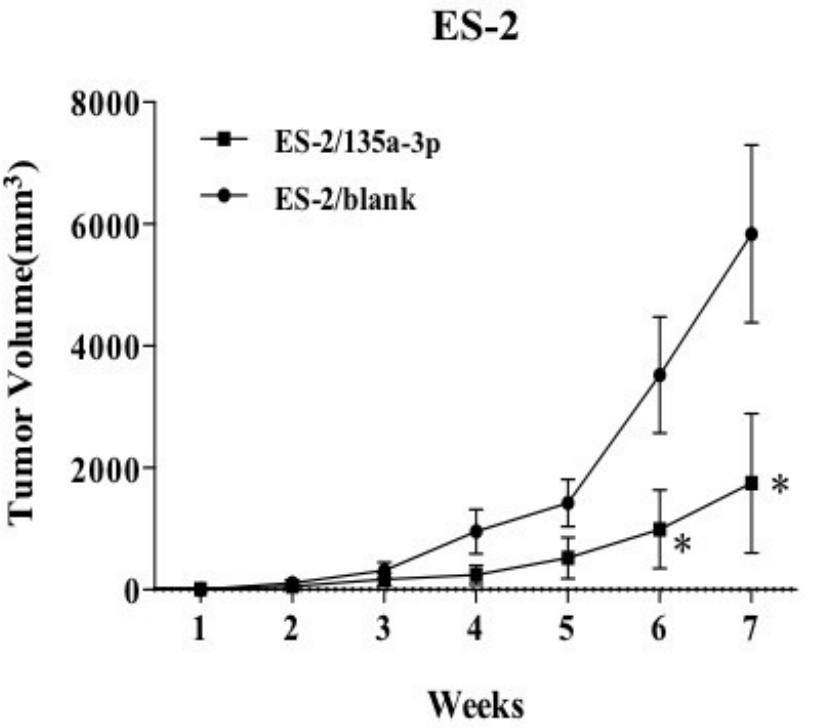
ES-2
8000
6000
4000
2000
0
Tumor Volume(mm3)
ES-2/135a-3p
ES-2/blank
*
*
1
2
3
4
5
6
7
Weeks

Figure 4

A

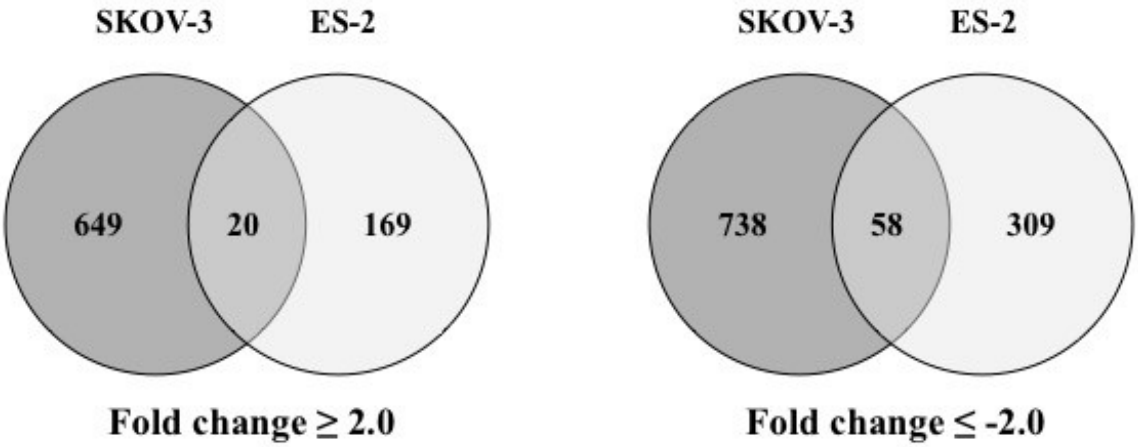
SKOV-3
ES-2
649
20
169
Fold change ≥ 2.0
SKOV-3
ES-2
738
58
309
Fold change ≤ -2.0

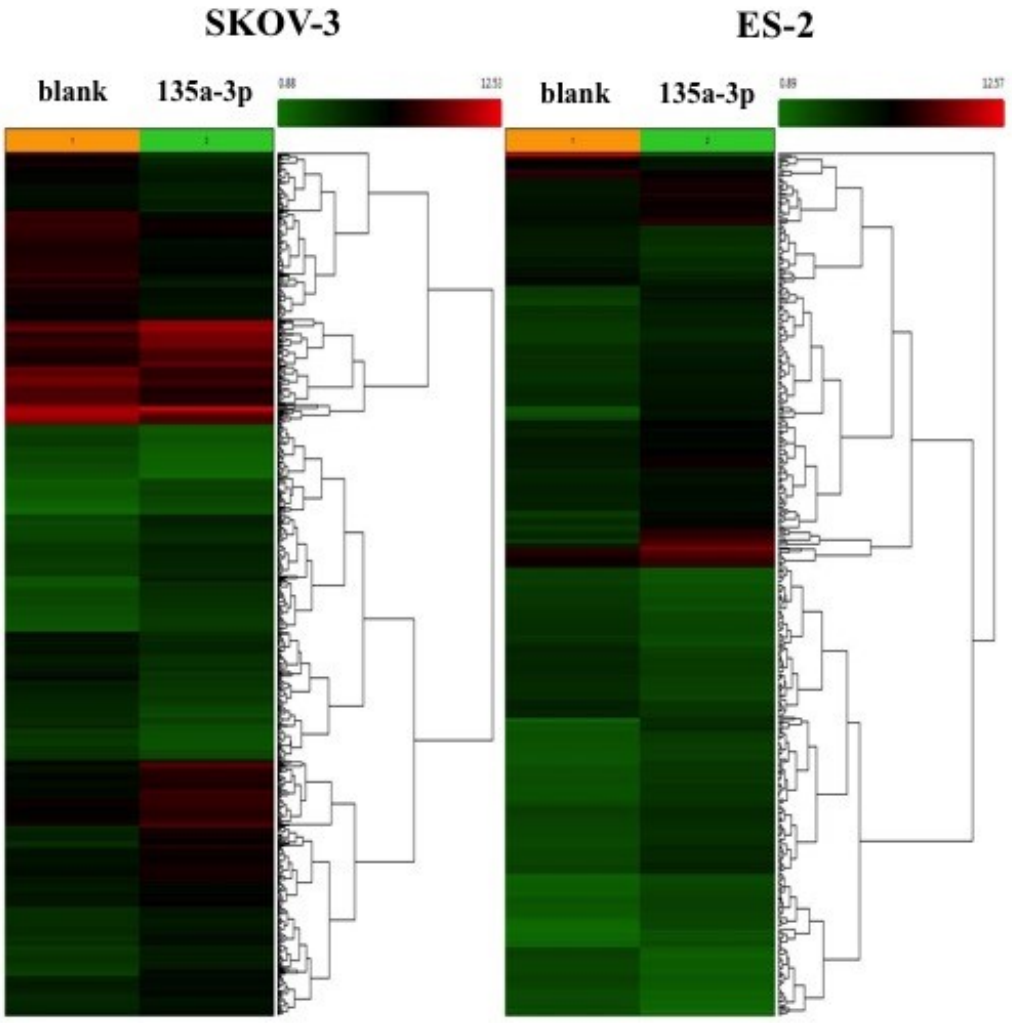
SKOV-3
blank
135a-3p
ES-2
blank
135a-3p

Figure 4

B

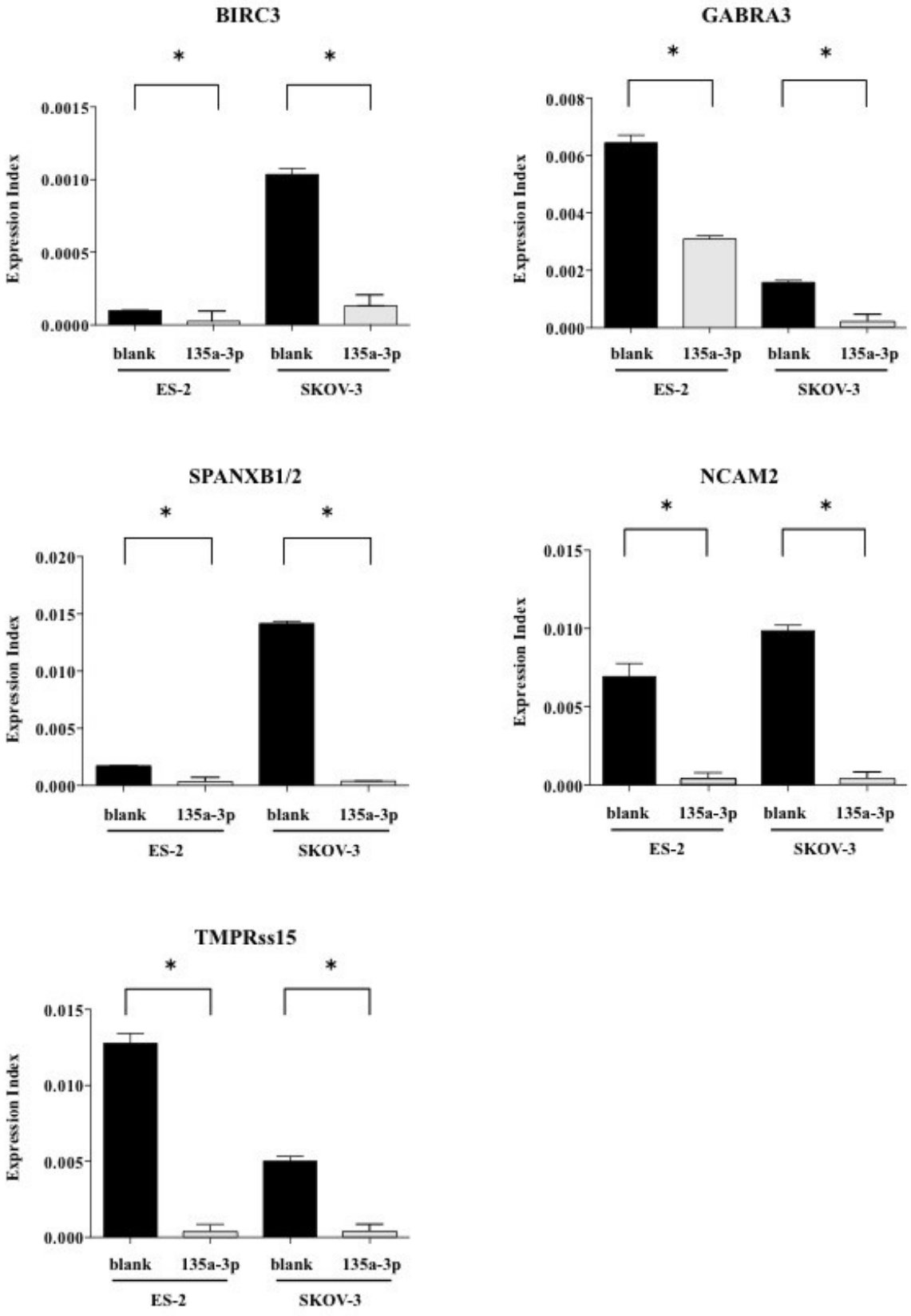
BIRC3
GABRA3
SPANXB1/2
NCAM2
TMPRss15
Expression Index
blank
135a-3p
ES-2
SKOV-3
*

Figure 5

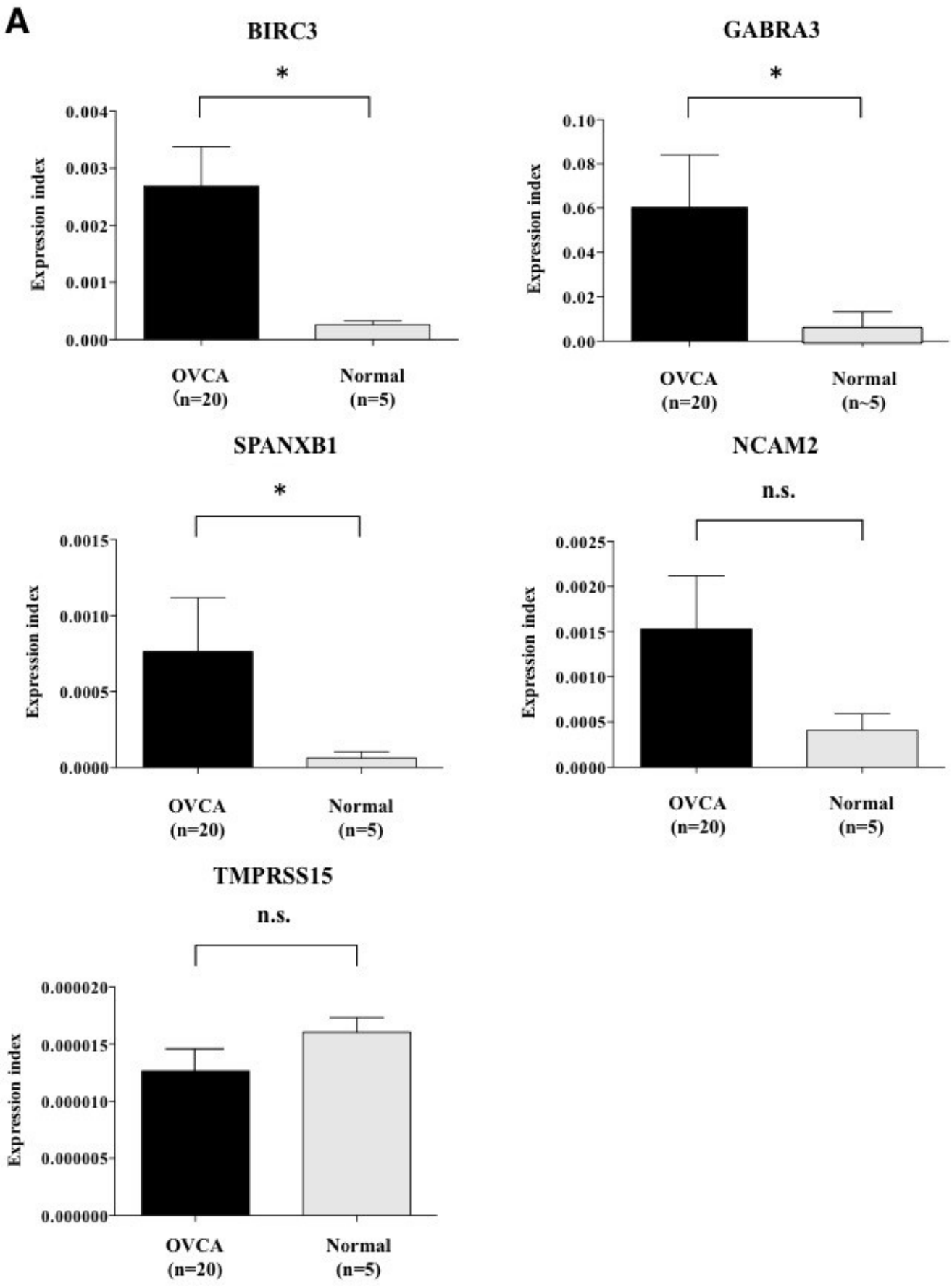
A
BIRC3
*
Expression index
0.004
0.003
0.002
0.001
0.000
OVCA (n=20)
Normal (n=5)
GABRA3
*
Expression index
0.10
0.08
0.06
0.04
0.02
0.00
OVCA (n=20)
Normal (n~5)
SPANXB1
*
Expression index
0.0015
0.0010
0.0005
0.0000
OVCA (n=20)
Normal (n=5)
NCAM2
n.s.
Expression index
0.0025
0.0020
0.0015
0.0010
0.0005
0.0000
OVCA (n=20)
Normal (n=5)
TMPRSS15
n.s.
Expression index
0.000020
0.000015
0.000010
0.000005
0.000000
OVCA (n=20)
Normal (n=5)

Figure 5

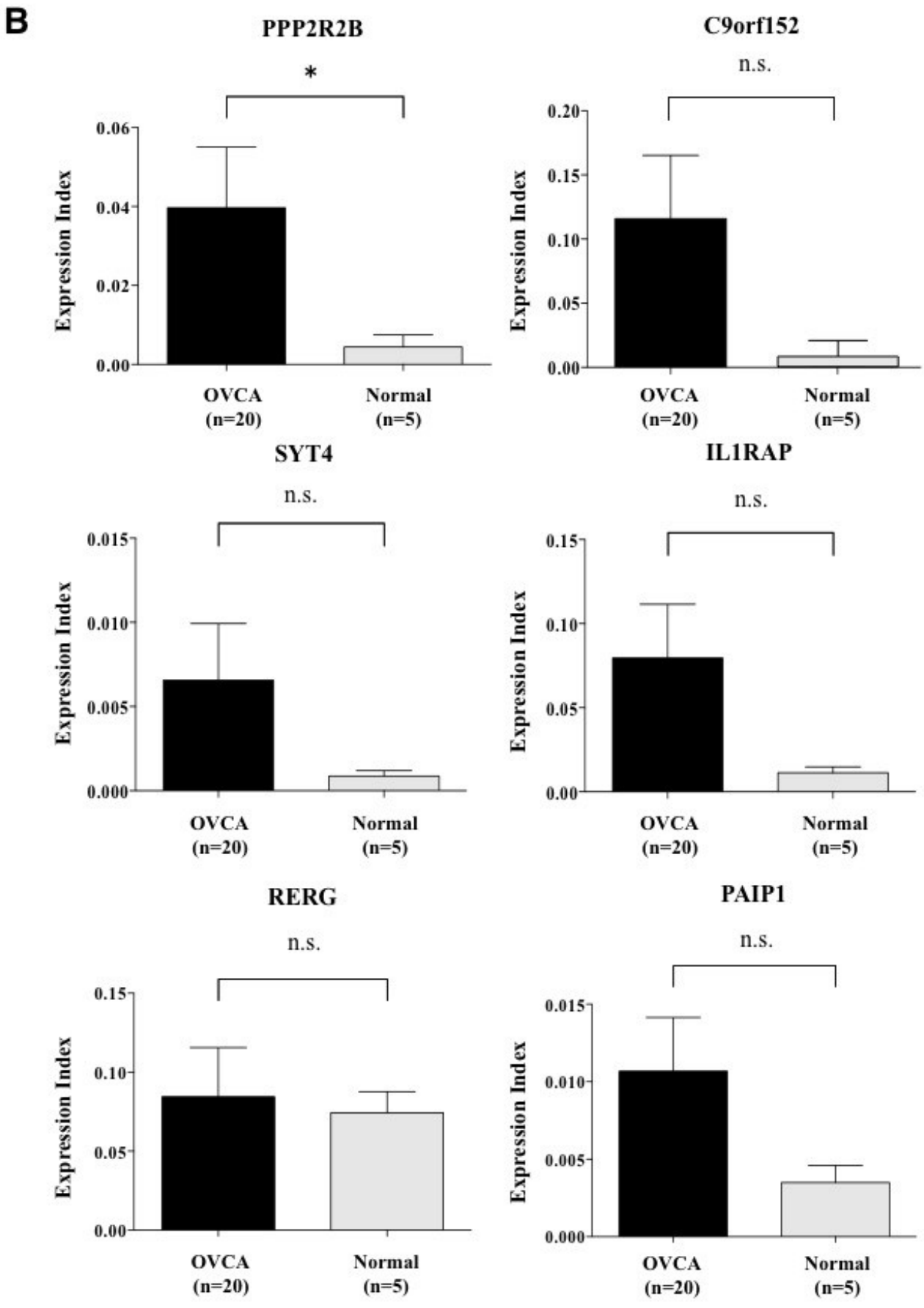
B
PPP2R2B
*
Expression Index
0.06
0.04
0.02
0.00
OVCA (n=20)
Normal (n=5)
C9orf152
n.s.
Expression Index
0.20
0.15
0.10
0.05
0.00
OVCA (n=20)
Normal (n=5)
SYT4
n.s.
Expression Index
0.015
0.010
0.005
0.000
OVCA (n=20)
Normal (n=5)
IL1RAP
n.s.
Expression Index
0.15
0.10
0.05
0.00
OVCA (n=20)
Normal (n=5)
RERG
n.s.
Expression Index
0.15
0.10
0.05
0.00
OVCA (n=20)
Normal (n=5)
PAIP1
n.s.
Expression Index
0.015
0.010
0.005
0.000
OVCA (n=20)
Normal (n=5)

Supplementary Figure 1

Alterations in the expression index of miR-135a-3p (A), miR-630 (B), or miR-1207 (C) in 98 patients with ovarian cancer.

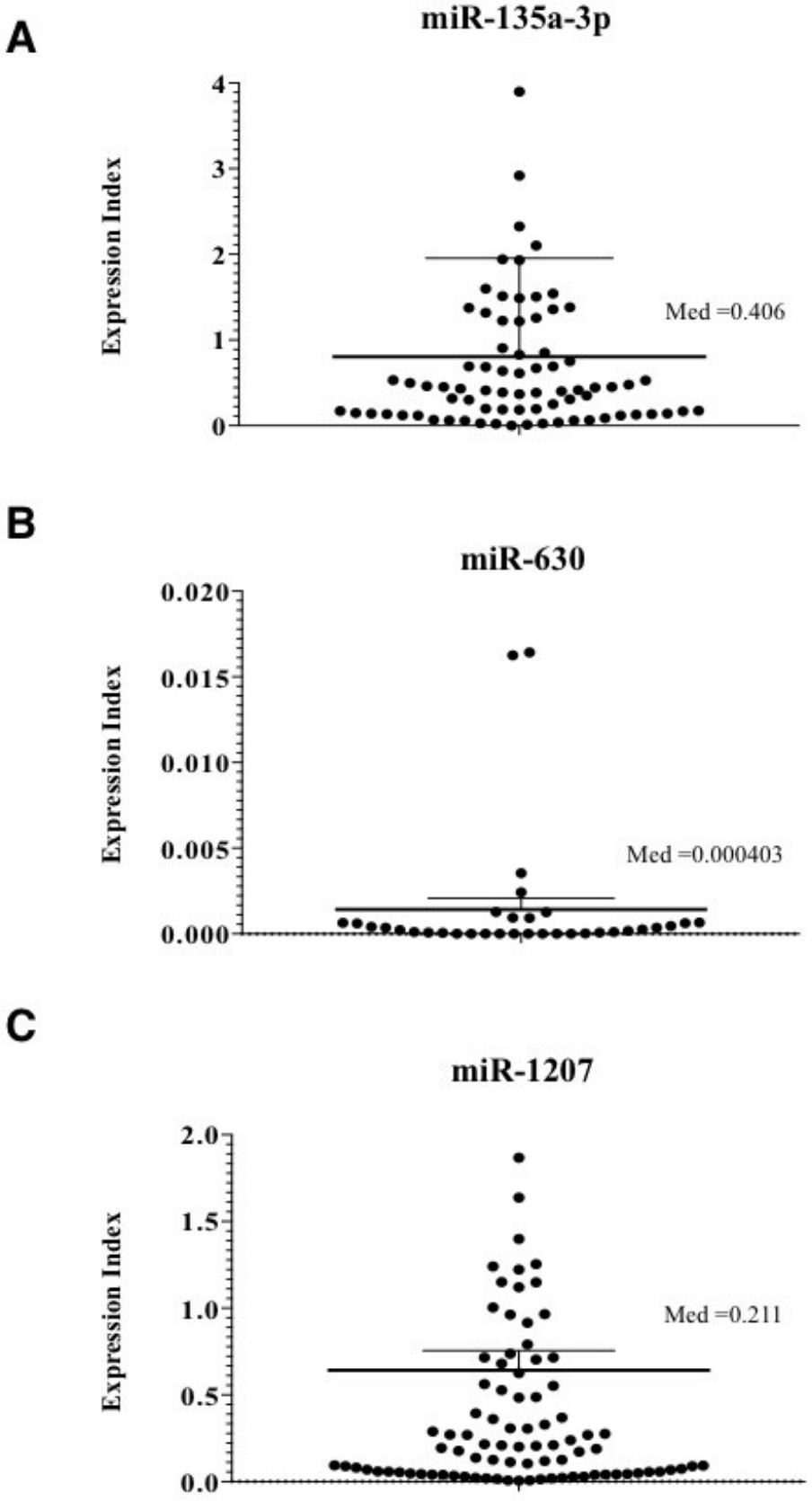

Supplementary Figure 2

Relationship between the expression index of miR-135a-3p and serum CA125 in 47 patients with ovarian cancer. R indicates the correlation index. (* P<0.05)

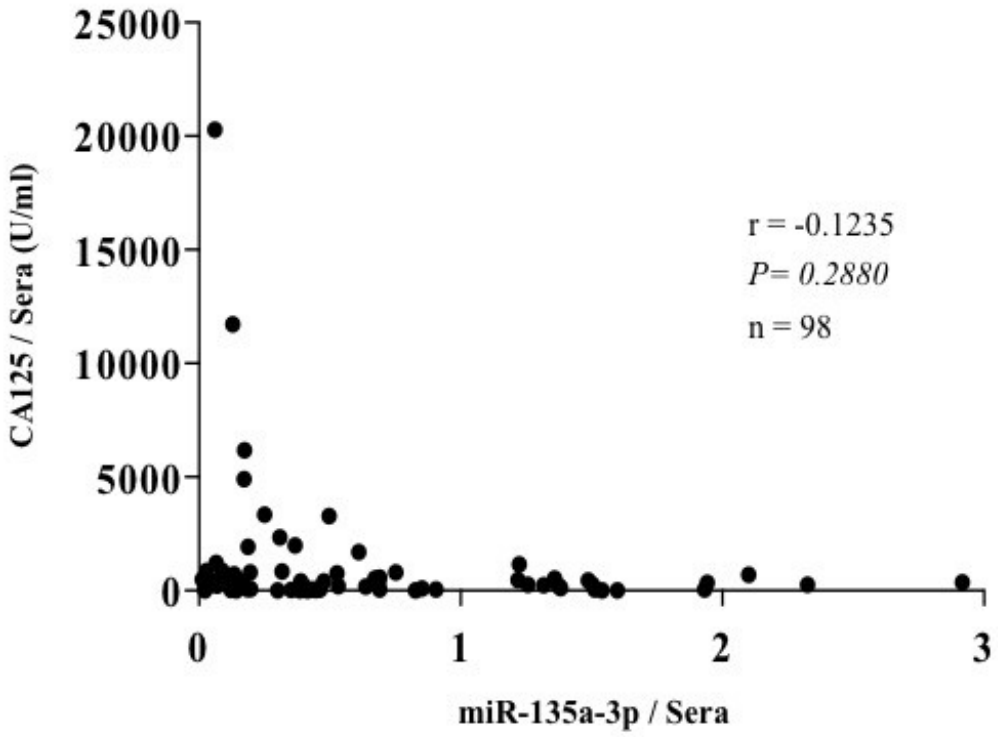

Supplementary Figure 3

Alterations in body weight of NOD/SCID mice with xenograft tumors of SKOV-3 or ES-2 cells transfected with miR-135a-3p or miR-blank. (* P<0.05)

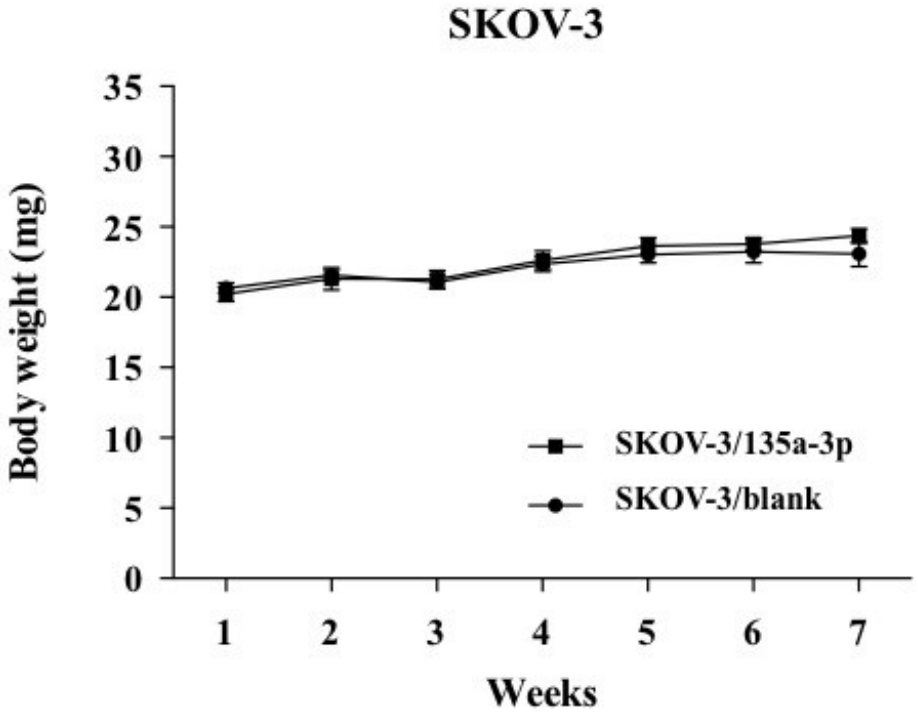

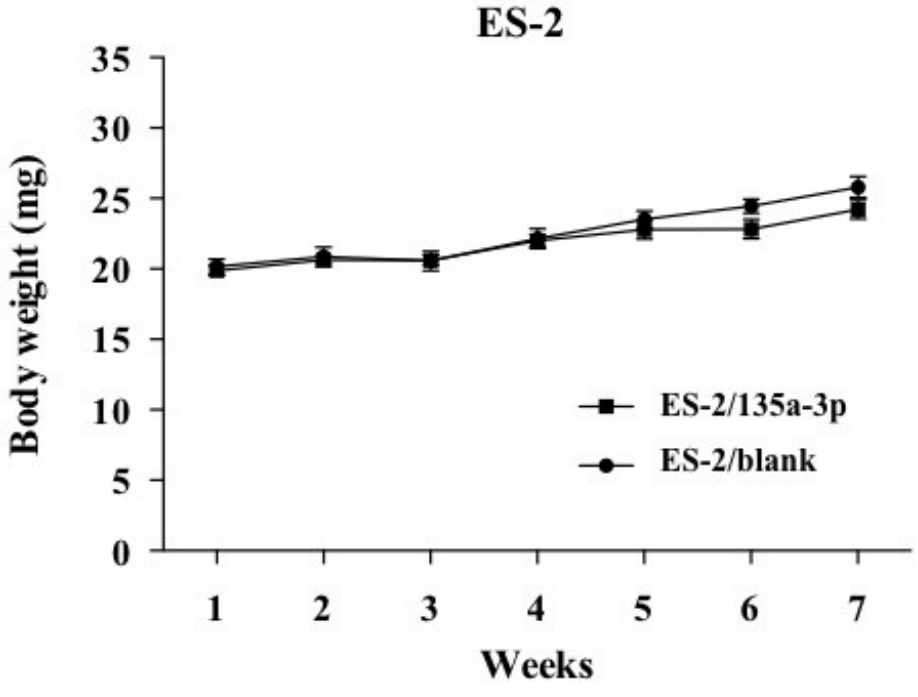

Supplementary Figure 4

Profiling of genes targeted by miR-135a-3p through prediction using Targetscan, miRDB, and miRanda.